Oct 26th, 12:00 AM

Shear Lag Effect on Bolted L-shaped Cold-formed Steel Tension Members

Chi-Ling Pan

Eighteenth International Specialty Conference on Cold-Formed Steel Structures

Orlando, Florida, U.S.A, October 26 & 27, 2006

Shear Lag Effect on Bolted L-Shaped Cold-Formed Steel Tension Members

Chi-Ling Pan

Abstract

This study is concentrated on the investigation of the shear lag effect on the cold-formed steel tension members. L-shaped specimens with different dimensions tested by using one-line or two-line bolted connections were discussed in this study. Based on the experimental results, it was found that there are quite discrepancy between the test results and the predicted values for the specimens with larger size of non-connected element. The comparison was made between the test results and predictions computed based on several specifications. Based on the experimental results, it was found that the tension strengths of test specimens predicted by the AISC Code (1999), which takes account of shear lag effect, are underestimated. The predictions according to AISI Specification (1996) and AS/NZS 4600 Code (1996) seem to be overestimated as comparing to the test results. The predicted values calculated according to the 2001 AISI Specification gives a better result for L-shaped tension members. It is also noted that there is quite discrepancy between the test results and the values predicted by British Standard (1998). It was also founded that the ratio of connection eccentricity to connection length, $\overline{x}$ /L, and the ratio of unconnected elements to connected elements, W_u/W_c, are the main factors which can mainly influence the tensile strength of angle sections. The tensile strength may be estimated by using the artificial neural network proposed by this study for the L-shaped sections under tension.

1. Introduction

Due to the variety of cross sectional shape for cold-form steel members, for the practical reason it is not normally possible or convenient to connect each element to the end connection. Therefore, the shear lag effect will be occurred for the member subjected to tension. According to the AISC Specification, a tension member can fail by reaching one of two limit states: (1)Excessive Deformation - the load on the member must be small enough that the stress in the cross section is less than the yielding stress of the steel; (2)Fracture – the load on the member must be small enough that the stress in

Professor, Dept. of Construction Engineering, Chaoyang University of Technology, 168, Gifeng E. Rd., Wufeng, Taichung County, Taiwan, R.O.C.

the effective net section is less than the tensile strength of the steel. The main factor considered in the AISC Specification (1999) for computing the effective net area is the shear lag effect. Shear lag effect occurs when some elements of the tension member are not connected. This effect reduces the strength of the member because the stresses distributed over the entire section are not uniform (Easterling and Giroux, 1993). The average value of stresses on the net section may thus be less than the tensile strength of the steel. The reduced strength of the member can be expressed as the efficiency of the net section. Research reported by Munse and Chesson (1963) suggests that the shear lag effect can be accounted for by using a reduced net area. Based on this assumption, AISC Specification (1999) states that the effective net area, A_e, of such a member is to be determined by multiplying its net area (if bolted or riveted) by a reduction factor U, that is, when the tension load is transmitted only by fasteners:

$$A_e = UA_n \tag{1}$$

where U = reduction factor = $1.0 - \bar{x}/L < 0.9$ (2)

$\bar{x}$ = connection eccentricity

L = length of the connection in the direction of loading

Due to the variety of cross sectional shapes for cold-formed steel members, it is not normally possible or convenient to connect each element to the end connection. Currently, the design formulas of the 1996 AISI Specification do not consider the effect of shear lag. So, as described in the AISI Specification, the nominal tensile strength (T_n) of axially loaded cold-formed steel tension members is simply determined by the net area of the cross section (A_n) and the yield stress of steel (F_y):

$$T_n = A_nF_y \tag{3}$$

When a bolted connection is used, the nominal tensile strength is further limited by the capacity specified in Specification Section E3.2 (1996). Based on the research finding by LaBoube and Yu (1995), design equations have been proposed and adopted in AISI Specification Supplement No.1 (1999) to estimate the influence of shear lag. The same design provisions are now included in Section E3.2 of Appendices A and C of the 2001 edition of the North American Specification for the use in the USA and Mexico. The design criteria for the channel and angle sections under axial tension load are listed as follows:

$$P_n = A_eF_u \tag{4}$$

where F_u = tensile strength of the connected part

A_e = UA_n, effective net area with U defined as follows:

U = for angle members having two or more bolts in the line of force = $1.0 - 1.20\bar{x}/L < 0.9$ but shall not be less than 0.4 (5)

$\bar{x}$ = connection eccentricity (distance from shear plane to centroid of the cross section)

L = length of the connection

In accordance with British Standard: Structural Use of Steelwork in Building – Part 5. Code of Practice for Design of Cold-Formed Sections (1998), the tensile capacity, P_t, of a plain channel can be determined from:

$$P_t = A_e p_y \tag{6}$$

where p_y = design strength, should be taken as Y_s (nominal yield strength) but not greater than $0.84U_s$ (nominal ultimate tensile strength); a_1 = the net sectional area of the connected leg; a_2 = the cross sectional area of the unconnected legs; and A_e = effective net area of the net section listed below:

$$A_e = \frac{a_1(3a_1 + 4a_2)}{(3a_1 + a_2)} \tag{7}$$

Equation (6) may only be used when the width to thickness ratios of the unconnected elements are less than 20.

Australian/New Zealand Standard: Cold-Formed Steel Structures (1996) gives formula similar to that in the AISC Specification as shown here as Equation (8). The nominal design tensile strength is determined by the smaller value of Equations 8a and 8b. Instead of using A_e, a term of $0.85K_tA_n$ is used in Equation (8b) to express the effective net area.

$$P_t = A_g f_y \tag{8a}$$

$$= 0.85k_tA_nf_u \tag{8b}$$

where A_g = gross area of cross section; A_n = net area of cross section; f_u = tensile strength used in design; f_y = yield stress used in design; and k_t = correction factor for distribution of forces.

Kulak and Wu (1997) conducted physical tests using single and double angle tension members to obtain the net sectional strength and thereby examine the shear lag effect. Developing from the tests, the prediction of ultimate load based on the failure mode is proposed by adding the ultimate strength of the critical section of the connected leg and the strength contributed by the critical section of the outstanding leg. Holcomb, LaBoube and Yu (1995) studied both angle and channel sections subjected to a tensile load parallel to their longitudinal axis. The primary intent of the test program was to determine the effect of shear lag. It was found that the geometric parameter (t/s') has an influence on the strength of bolted connections of cold-formed steel members. Pan (2004) tested a series of bolted cold-formed channel sections to study the shear lag effect. Pan concluded that the ratio of connection eccentricity to connection length, $\overline{x}/L$, and the ratio of unconnected elements to connected elements, W_u/W_c, might be the two factors which can mainly influence the tensile strength of channel sections.

2. Experimental Study

The test material used in this study is SSC400 sheet steel specified in Chinese National Standard (1994) with a nominal ultimate tensile strength of 41 kgf/mm^2 (400 N/mm^2) and up. Two different thicknesses, 2.3 mm and 3.2 mm, of sheet steels were used to fabricate the specimens. The material properties of both steels were obtained by tensile coupon tests. The yield stress and tensile strength of the 3.2 mm–thick sheet steel are 314.10 MPa and 434.24 MPa, respectively. And for the 2.3 mm–thick sheet steel, the yield stress and tensile strength are 324.20 MPa and 438.53 MPa, respectively. The fasteners used to connect the L-shaped specimens were ASTM A325T high strength bolts.

2.1 Specimens

For the selection of the dimensions of cross sections, the specimens were designed to have a failure type of fracture on the net cross section, so that the shear lag effect can be evaluated. The specimens were also numerically verified to avoid bearing failure of cross section and bearing failure and shear failure of the bolt. Three groups of specimens were used to conduct in this study:

Group A: L-shaped section with a nominal connected leg width of 100 mm and nominal unconnected leg width of 50 mm. (AA-100×50×3.2 and AB-100×50×2.3)

Group B: L-shaped section with a nominal connected leg width of 100 mm and nominal unconnected leg width of 100 mm. (BA-100×100×3.2 and BB-100×100×2.3)

Group C: L-shaped section with a nominal connected leg width of 100 mm and nominal unconnected leg width of 120 mm. (CA-100×120×3.2 and CB-100×120×2.3)

Two L-shaped sections were assembled back to back by using four high-strength bolts. A total of 12 pairs of sections were connected using two bolts in two lines of force. In addition, another 12 pairs of sections were connected using four bolts in one line of force. The spacing between the centers of bolt holes, 40 mm, was chosen to be larger than three times the bolt diameter. The distance from the end of the specimen to the nearest center of bolt hole, 20 mm, was designed to be larger than 1.5 times the bolt diameter according to the AISI Specification. All holes were drilled to 14.3 mm in diameter, and were accommodated with 12.7 mm diameter ASTM A325T bolts as a bearing-type connection.

2.2 Test Setup

A tensile testing machine with a capacity of 50 tons was used to conduct all the tests. The configuration of test setup is shown in Figure 1. Two L-shaped sections in same group were assembled back to back by using four bolts and were pulled to failure in the opposite direction. The

bearing-type connection was adopted in the bolt assembly as specified in Section E3 of the AISI Specification. During the test, two LVDTs (Linear Variable Differential Transformer) were used to measure the axial deformation for each specimen. Strain gages were also attached on the surfaces of specimens to monitor the strain variations through the test. Figure 2 shows the placements of strain gages on the schematic unfolded specimens connected using two bolts in two lines of force. After the test, a statistical analysis was performed to study the difference between the predicted value and the test result for each specimen.

3. Evaluation of Experimental Data

The failure mode of net section fracture was observed for the specimens connected using two bolts in two lines of force. A typical failure photo is shown in Figure 3. On the other hand, a combined tearing and bearing failure was found for the specimens connected using four bolts in one line of force. As expected, the stress distributions in the cross section of specimen are not uniformed due to the shear lag effect. Figures 4 shows the stress distributions in the two cross sections under a loading stage $1/4A_gF_y$ for the specimen BB-3. Due to the axial loading, tensile stresses were observed in most segments at two different cross sections. Some segments were affected by the eccentricity of connection, therefore, compressive stresses were found in the edge area of unconnected elements as can be seen in Figure 4. In this study, the comparisons were only made between the test results and predictions computed based on several specifications for the specimens having net section failure (specimens connected using two bolts in two lines of force) in order to study the shear lag effect. Table 1 summaries the measured dimensions of the cross sections for the specimens having the failure mode of net section fracture. In Table 1,H = overall width of connected leg; B = overall width of unconnected leg; t = thickness of steel; R = inside radius of corner; and A_g = gross area

3.1 Comparison with AISI Specification

The predicted values calculated based on the 1996 and 2001 AISI Code (P_{n1} and P_{n2}) and tested values for the specimens are listed in Table 2. The computed tensile strength, P_{n1}, is based on considering the yield stress occurred uniformly in the net section. The ratios of tested to computed tensile strengths (P_{n1}) for each specimen (column (5) of Table 2) are all smaller than unity varying from 0.566 to 0.934. Due to ignoring connection eccentricity, the predictions of tensile capacity using the 1996 AISI Specification for a member under axial tension seems to be over estimated. The predicted values calculated according to the 2001 AISI Specification are listed in column (2) of Table 2. Equation (5) used to compute the predicted values was established mainly based on the consideration of the shear lag effect. It was observed from column (6) of Table 2 that the mean and

standard deviation of the tested to computed tensile strengths can be improved. It seems that the amended formula (Equation (5)) gives a better result for L-shaped tension members having two bolts in the line of force.

3.2 Comparison with BS Specification

The comparisons between test values and the computed tensile strength based on the BS Specification are listed in Table 3. The computed tensile strengths listed in Table 3 were calculated according to Equation 6. It can be seen from Table 3 that the mean value of P_{test}/P_n ratios (tested to computed tensile strength ratios) is 0.884 with a standard deviation of 0.110. The scatter between the tested and predicted values of tensile strength is probably due to the lack of consideration of the connection length and type, even though the areas of connected and unconnected elements of the member are considered in the calculation of tensile strength for the BS Specification.

3.3 Comparison with AS/NSZ Specification

The predicted tensile strength for each specimen according to the AS/NSZ Specification are listed in column (2) of Table 4. It was observed from Table 4 that the ratios of tested to computed tensile strength for each specimen are between 0.643 and 0.955. For the specimens with larger width of unconnected leg, the ratios varied from 0.643 to 0.695. Thus the tensile strength is much overestimated for the specimens with larger width of unconnected leg tested in this study. The equation (Equation 7) for predicting the tensile strength of a tension member is quite simple and convenient to use. However, failure to consider the connection length may have caused the discrepancies between the tested and computed values of tensile strength.

3.4 Comparison with AISC Specification

Table 5 compares tested tensile strengths with values according to the AISC Specification. The predicted tensile strength for each specimen is determined by P_{n2} and listed in column (2) of Table 5. The range of values for the ratio of tested to computed values for the specimens is from 1.339 to 2.851. It can be seen from Table 5 that the mean value of P_{test}/P_n ratios (tested to computed tensile strength ratios) is 1.894 with a standard deviation of 0.591. The computed values calculated based on the AISC Specification provide bad correlation with the test results. Contrary, the current AISC Specification is a relatively good predictor of the tensile strength for the channel tension members (Pan, 2004).

4. Model Construction

Because the axial force in the main portion of the L-shaped member is eccentric with respect to the connected ends, bending can also be present.

This portion of study is concentrated on proposing a model that is more efficient than the currently used ones. The efficiency factor proposed here is based on the following factors: (1)effect of bolts on the net section strength; (2)connection eccentricity in horizontal direction; (3)connection eccentricity in vertical direction; and (4)ratio of unconnected length to connected length.

As shown in Figure 5, the force along the bolt line causes torque about the centroid of the section. This torque can be split into 2 components acting in the horizontal and vertical planes. The bending stresses developed in the member to oppose these external torques results in non-uniform stress distribution in the section. Analyzing experimental results have shown that the vertical and horizontal distance between the bolt line and the centroid line has a significant role in determining the ultimate strength of the member, and they are represented by x_1 and x_2 respectively in the proposed shear lag factor. The x_1 represents the distance from the shear plane to the centroid of the whole cross section, meanwhile, the x_2 represents the distance between centroid of shaded cross section and the center of bolt hole close to the corner as can be seen in Figures 6(a) and 6(b), respectively.

Artificial neural networks (ANNs) are new computational tools that have found extensive utilization in solving many complex real-world problems. The attractiveness of ANNs comes from their remarkable information processing characteristics pertinent to nonlinearity, high parallelism, fault and noise tolerance, and learning and generalization capabilities. ANNs can be defined as structures comprised of densely interconnected adaptive simple processing elements (called artificial neurons or nodes) that are capable of performing data processing and knowledge representation (Nelson, 1990, Schalkoff, 1997). A vast number of networks, new or modifications of existing ones, are being constantly developed. Pham (1994) estimated that over 50 different ANN types exist. Among them, Bacppropagation (BP) networks are the most popular and versatile network in solving complex problems. A backpropagation network is an MLP consisting of (1) an input layer with nodes representing input variables to the problem; (2) an output layer with nodes representing the dependent variables (i.e., what is being modeled); and (3) one or more hidden layers containing nodes to help capture the nonlinearity in the data. In a BP, the data are fed forward into the network without feedback. The neurons in BPs can be fully or partially interconnected. These networks are so versatile and can be used for data modeling, classification, forecasting, control, data and image compression, and pattern recognition (Hanson, 1995).

In this research, BPs are used to construct the mapping models. Experiments were conducted using ANN toolbox under Matlab 6.1. The

structure of BP with Levenberg-Marquardt training algorithm is shown in Figure 7, which consists of input layer, two hidden layers, and an output layer. The TANSIG function was used as the transfer function in two hidden layers to conduct the non-linear transformation between layers. For the output layer, PURELIN function (linear mapping between layers) was adopted. The initial weight was randomly generated by the toolbox. According to Pan's recommendation (2004), the ratio of connection eccentricity to connection length, $\overline{x}$ /L, and the ratio of unconnected elements to connected elements, W_u/W_c, are the two factors which can mainly influence the tensile strength of channel sections. Therefore, the input vectors used to compute the reduction factor (U) are x_1/L, x_2/L, and W_u/W_c. The target values are the tested ultimate load of specimens including the data conducted in this study and Holcomb's test results (1995). After 10,000 epochs, the mean squared error (MSE) was reaching 0.028. In order to guarantee a convergence, the learning rate was set a small value 0.001 with dynamically modification. The learning result is listed in Table 6. The result shows that the constructed BP performed well in data mapping.

5. Conclusions

In order to investigate the effect of shear lag on the C-shaped cold-formed steel sections, four groups of specimens were tested under tension. A total of 12 pairs of sections were tested in this study. Based on the test specimens having the failure mode of net section fracture, the following conclusions can be drawn for the L-shaped cold-formed steel tension members:

1. From observing the strain readings in the test, it is apparent that the stress distribution over the entire section of the specimen is not uniform. The stresses in the connected leg are larger than the stresses in the unconnected leg. Thus, the effect of shear lag is demonstrated, and the effect of eccentricity noted
2. It was found that the tensile strengths of test specimens predicted by the AISC Code (1999), which takes into account the shear lag effect, provide bad correlation with the test results. The predictions according to AISI Specification (1996) and AS/NZS Standard (1996) seem to be overestimated as compared to the test results. However, the predicted values calculated according to the 2001 AISI Specification gives a better result for L-shaped tension members. It was also noted that there is quite a discrepancy between the test results and the values predicted by British Standard (1998). The scatter between the tested and predicted values of tensile strength is probably due to the lack of consideration of the connection length and type.
3. Artificial neural network might be a computational tool that can be used to predict the strength of cold-formed steel tensile member. Bacppropagation network is adopted to construct the mapping models

in this study. The result shows that the constructed BP performed well in data mapping. However, more test data for the angle sections need to be investigated to see whether they also meet this finding.

In summary, the tensile strength of a L-shaped cold-formed steel section can be influenced by the shear lag effect. The cross section is termed not fully effective when it is not connected through all elements of the cross section. The nonlinearity regression analysis that consider the ratio of connection eccentricity to connection length, $\overline{x}$ /L, and the ratio of unconnected elements to connected elements, W_u/W_c, as the parameters is needed to be conducted in the future work.

References

1. American Institute of Steel Construction (AISC), "Load and Resistance Factor Design Specification for Structural Steel Buildings," Chicago, Ill., 1999.
2. American Iron and Steel Institute (AISI), "1996 Edition of the Specification for the Design of Cold-Formed Steel Structural Members," Washington, DC, 1996.
3. American Iron and Steel Institute (AISI), "North American Specification for the Design of Cold-Formed Steel Structural Members, " 2001 Edition, Washington, DC, 2001.
4. British Standard Institute (BSI), "British Standard: Structural Use of Steelwork in Building- Part 5. Code of Practice for Design of Cold-formed Thin Gauge Sections," London, 1998.
5. Chinese National Standard (CNS), "Light Gauge Steels for General Structure," Bureau of Standards, Metrology and Inspection, Ministry of Economic Affairs, CNS 6183, G3122, 1994.
6. Easterling, W. Samuel, and Giroux, Lisa Gonzalez, "Shear Lag Effects in Steel Tension Members," *Engineering Journal*, American Institute of Steel Construction, Inc., Vol. 30, No. 3, pp77-89, 1993.
7. Hanson, S.J., Backpropagation: some comments and variation. Macmillan, New York, 1995.
8. Kulak, G.L. and Wu, E.Y., "Shear Lag in Bolted Angle Tension Members," *Journal of Structural Engineering*, ASCE, Vol. 123, No. 9, pp1144-1152, 1997.
9. Holcomb, B.D., Yu, W.W., and LaBoube, R.A., "Tensile and Bearing Capacities of Bolted Connections," 2nd Summary Report, Civil Engineering Study 95-1, University of Missouri-Rolla, 1995.
10. LaBoube, R.A. and Yu, W.W., "Tensile and Bearing Capacities of Bolted Connections," Final Summary Report, Civil Engineering Study 95-6, University of Missouri-Rolla, 1995.

11. Munse, W.H., and Chesson, E. Jr., "Riveted and Bolted Joints: Net Section Design," *Journal of the Structure Division*, Proc. ASCE, Vol.89, No. ST 1, pp107-126, 1963.
12. Nelson, M. and Illingworth, W.T., A Practical Guide To Neural Nets, Addison-Wesley, Reading, MA, 1990.
13. Pan, C.L., "Prediction of the Strength of Bolted Channel Sections in Tension," *Journal on Thin-walled Structures*, Elsevier Science Limited. Vol.42, pp1171-1198, 2004.
14. Pham, D.T., Neural networks in engineering. In: Rzevski, G. et al. (Eds.), Applications of Artificial Intelligence in Engineering IX, AIENG/94, Proceedings of the 9th International Conference. Computational Mechanics Publications, Southampton, pp. 3–36, 1994.
15. Schalkoff, R.J., Artificial Neural Networks, McGraw-Hill, New York, 1997.

Notation

A_{cn} = net area of the connected leg at the critical section
A_e = effective net area of the net section
A_g = gross area of cross section
A_n = net area of cross section
A_o = area of the outstanding leg (gross area)
a_1 = the net sectional area of the connected leg
a_2 = the cross sectional area of the unconnected legs
F_u = tensile strength of the connected part
F_y = yield strength of the material
f_u = tensile strength used in design
f_y = yield stress used in design
k_t = correction factor for distribution of forces
L = length of the connection in the direction of loading
P_n = computed tensile strength
P_{pred} = predicted tensile strength
P_t = tensile capacity
P_{ult} = tested ultimate strength
p_y = design strength
T_n = nominal tensile strength
t = thickness of steel sheet
U = reduction factor
Y_s = nominal yield strength
s' = connected width + $\overline{x}$
x_1 = distance from the shear plane to the centroid of the whole cross section
x_2 = distance between centroid of shaded cross section and the center of bolt hole close to the corner
$\overline{x}$ = connection eccentricity

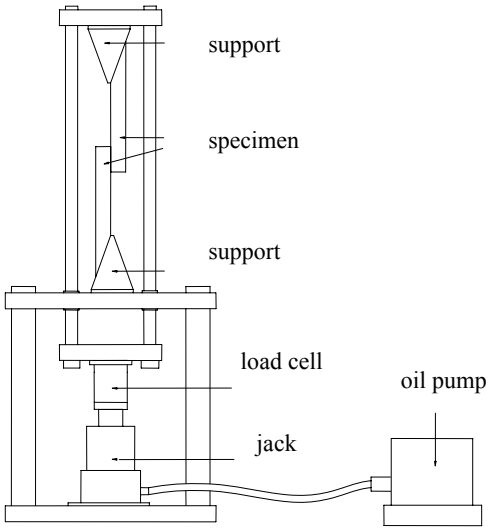

Figure 1 Configuration of Test Setup

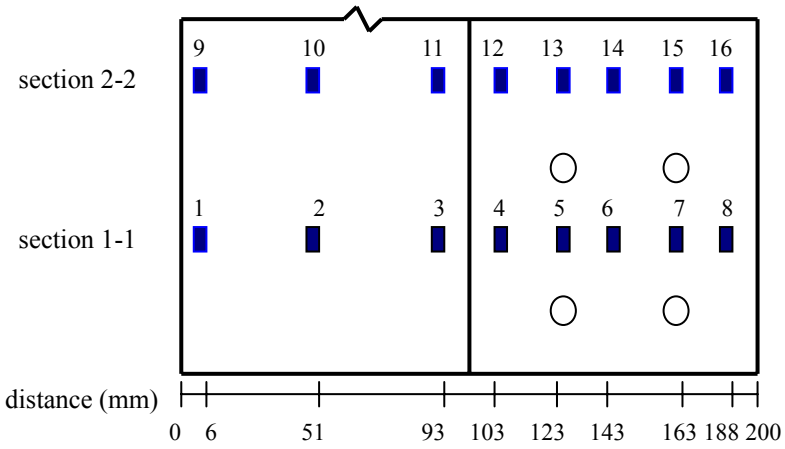

Figure 2 Locations of Strain Gages on the Schematic Unfolded Specimen

Figure 3 Typical Failure of a Specimen

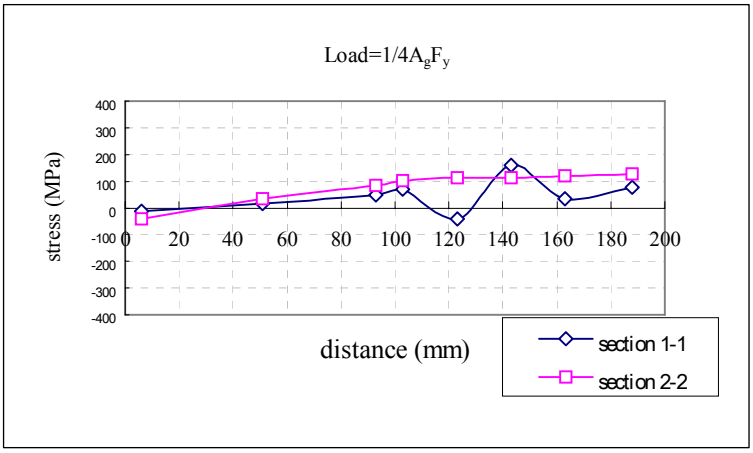

Figure 4 Stress Distributions at Three Cross Sections for Specimen BB-2 under the Load Reaching $(P_u)_{test}$

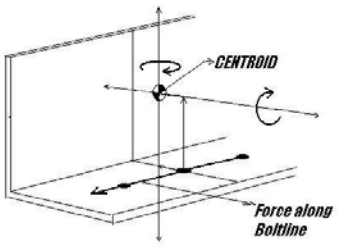

Figure 5 Torques Caused by Connection Eccentricity

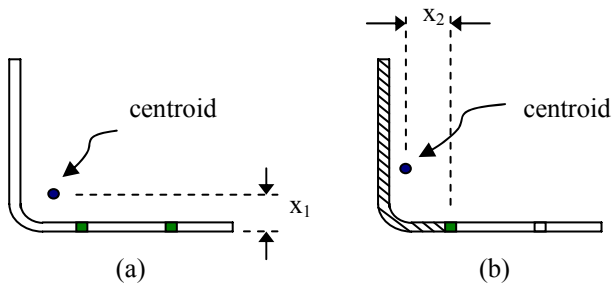

Figure 6 Schematic Plot of Connection Eccentricity $\overline{x}$

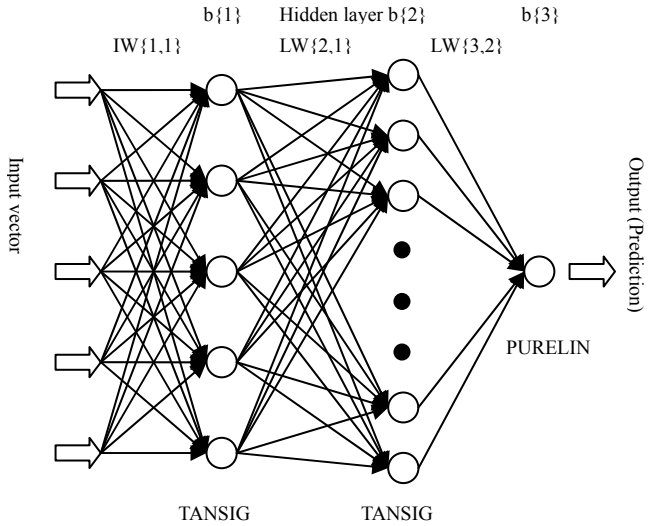

Figure 7 The structure of BP using Levenberg-Marquardt Algorithm

Table 1 Nominal Dimensions of Cross Sections

spec. no.	H(mm)	B(mm)	t(mm)	R(mm)	Ag(mm^2)
AA-1	99.99	50.79	3.20	2.28	465.75
AA-2	99.99	50.88	3.20	2.15	467.38
AB-1	99.94	50.75	2.30	1.76	338.43
AB-2	99.97	50.89	2.30	2.04	338.54
BA-1	100.11	100.79	3.20	1.85	627.90
BA-2	100.03	100.93	3.20	2.04	627.85
BB-1	99.98	100.80	2.30	2.13	453.28
BB-2	99.96	100.68	2.30	1.68	453.40
CA-1	100.09	120.52	3.20	2.01	690.75
CA-2	100.22	120.63	3.20	2.19	688.60
CB-1	99.92	119.44	2.30	2.44	495.69
CB-2	100.02	119.30	2.30	1.70	496.32

Table 2 Comparison of Test Results with AISI Specification

specimen no.	P_{n1} (kN) (1)	P_{n2} (kN) (2)	P_{test} (kN) (3)	P_{test}/P_{n1} (4)	P_{test}/P_{n2} (5)
AA-1	120.76	118.46	109.78	0.909	0.927
AA-2	121.28	118.77	109.70	0.905	0.924
AB-1	90.11	87.66	84.12	0.934	0.960
AB-2	90.14	87.69	82.50	0.915	0.941
BA-1	171.69	94.95	115.09	0.673	1.212
BA-2	171.67	94.93	110.93	0.646	1.169
BB-1	127.34	68.90	85.28	0.670	1.238
BB-2	127.38	68.92	80.89	0.635	1.174
CA-1	191.44	105.86	115.79	0.605	1.094
CA-2	191.00	105.62	108.17	0.566	1.024
CB-1	141.09	76.34	84.59	0.600	1.108
CB-2	141.30	76.45	82.97	0.587	1.085
mean				0.720	1.071
standard deviation				0.148	0.114

Note: $P_{n1}= A_nF_y$, $P_{n2}= (1.0\text{-}1.20\,\overline{x}/L)A_nF_u$

Table 3 Comparison of Test Results with BS Specification

specimen no.	P_n (kN) (1)	P_{test} (kN) (2)	P_{test}/P_n (3)
AA-1	106.99	109.78	1.026
AA-2	107.41	109.70	1.021
AB-1	80.65	84.12	1.043
AB-2	80.58	82.50	1.024
BA-1	134.25	115.09	0.857
BA-2	134.01	110.93	0.828
BB-1	100.21	85.28	0.851
BB-2	100.51	80.89	0.805
CA-1	142.22	115.79	0.814
CA-2	141.69	108.17	0.763
CB-1	105.64	84.59	0.801
CB-2	106.36	82.97	0.780
mean			0.884
standard deviation			0.110

Note: $P_n= A_ep_y$

Table 4 Comparison of Test Results with AS/NZS Specification

specimen no.	P_{n1} (kN) (1)	P_{n2} (kN) (2)	P_{test} (kN) (3)	P_{test}/P_{n2} (4)
AA-1	149.41	120.60	109.78	0.910
AA-2	150.02	121.14	109.70	0.906
AB-1	111.43	88.06	84.12	0.955
AB-2	111.47	88.10	82.50	0.936
BA-1	200.44	171.50	115.09	0.671
BA-2	200.42	171.47	110.93	0.647
BB-1	148.66	124.45	85.28	0.685
BB-2	148.70	124.48	80.89	0.650
CA-1	220.18	168.72	115.79	0.686
CA-2	219.66	168.34	108.17	0.643
CB-1	162.42	121.67	84.59	0.695
CB-2	162.63	121.85	82.97	0.681
mean				0.755
standard deviation				0.128

Note: $P_{n1}= A_gF_y$, $P_{n2}= 0.85k_tA_nf_u$

Table 5 Comparison of Test Results with AISC Specification

specimen no.	P_{n1} (kN) (1)	P_{n2} (kN) (2)	P_{test} (kN) (3)	P_{test}/P_{n2} (4)
AA-1	149.41	69.49	109.78	1.580
AA-2	150.02	69.77	109.70	1.572
AB-1	111.43	49.91	84.12	1.685
AB-2	111.47	49.89	82.50	1.654
BA-1	200.44	81.59	115.09	1.411
BA-2	200.42	81.16	110.93	1.367
BB-1	148.66	60.10	85.28	1.419
BB-2	148.70	60.40	80.89	1.339
CA-1	220.18	40.61	115.79	2.851
CA-2	219.66	40.30	108.17	2.684
CB-1	162.42	32.16	84.59	2.630
CB-2	162.63	32.76	82.97	2.533
mean				1.894
standard deviation				0.591

Note: $P_{n1} = A_gF_y$, $P_{n2} = A_eF_u$

Table 6 Comparison of Test Results with BP Network

Test Data from This Study							
specimen no.	P_{test} (kN)	P_{pred} (kN)	P_{test}/P_{pred}	specimen no.	P_{test} (kN)	P_{pred} (kN)	P_{test}/P_{pred}
AA-1	109.78	109.76	1.000	BB-1	85.28	85.28	1.000
AA-2	109.70	109.77	0.999	BB-2	80.89	80.89	1.000
AB-1	84.12	84.11	1.000	CA-1	115.79	115.79	1.000
AB-2	82.50	82.51	1.000	CA-2	108.17	108.17	1.000
BA-1	115.09	115.09	1.000	CB-1	84.59	84.59	1.000
BA-2	110.93	110.94	1.000	CB-2	82.97	82.97	1.000
Test Data from Holcomb's Research							
specimen no.	P_{test} (kN)	P_{pred} (kN)	P_{test}/P_{pred}	specimen no.	P_{test} (kN)	P_{pred} (kN)	P_{test}/P_{pred}
LBN11-1	15.79	15.88	0.994	LCN11-1	19.57	19.54	1.002
LBN11-2	16.19	15.98	1.013	LCN11-2	20.02	20.02	1.000
LBN11-3	15.92	16.06	0.991	LCN11-3	20.91	20.93	0.999
LBN12-1	17.93	18.48	0.970	LCN12-1	21.93	21.93	1.000
LBN12-2	19.30	18.49	1.044	LCN12-2	22.82	22.81	1.000
LBN12-3	18.24	18.50	0.986	LCN13-1	29.80	29.80	1.000
LBN13-1	25.27	25.27	1.000	LCN13-2	31.71	31.71	1.000
LBN13-2	24.38	24.37	1.000	LCN31-1	58.49	58.49	1.000
LBN31-1	48.97	48.97	1.000	LCN31-2	56.71	56.71	1.000
LBN31-2	48.26	48.26	1.000	LCN32-1	62.94	62.94	1.000
LBN32-1	51.95	51.96	1.000	LCN32-2	60.18	60.18	1.000
LBN32-2	56.05	56.04	1.000	LCN33-1	88.29	88.30	1.000
LBN33-1	80.87	80.87	1.000	LCN33-2	90.87	90.87	1.000
LBN33-2	79.62	79.62	1.000				

Note: P_{prep} represents the values computed based on BP network model.